Available online at www.sciencedirect.com
ScienceDirect
Journal of Sound and Vibration 306 (2007) 74–90
JOURNAL OF SOUND AND VIBRATION
www.elsevier.com/locate/jsvi

Performance and reliability of semi-active equipment isolation

Henri P. Gavin[a], Anton Zaicenco[b,*]

[a]*Department of Civil and Environmental Engineering, Duke University, P.O. Box 90287, Durham, NC 27708-0287, USA*
[b]*Institute of Geophysics and Geology, Moldavian Academy of Sciences, Str. Academiei 3, MD-2028 Chisinau, Moldova*

Received 9 February 2006; received in revised form 11 May 2007; accepted 22 May 2007
Available online 3 July 2007

Abstract

This study examines the performance and reliability of passive and semi-active damping in equipment isolation systems for earthquake protection. Performance and reliability measures are the peak accelerations sustained by the equipment and the peak displacements of the isolation system. A new hybridization of two previously studied semi-active control rules regulates the damping in the semi-active isolation system. A parameter study identifies suitable values for the stiffness and damping parameters of the passive isolation system, and feedback control constants for the semi-active equipment isolation and compares the performance for a set of historical earthquakes and for a set of different building models. The reliability of passive and semi-active equipment isolation systems is assessed separately for four historic earthquakes and in regards to uncertainties in the isolation system. The reliability assessment makes use of a polynomial metamodel of the responses as a function of the relevant random variables. Results illustrate the performance limitations of passive isolation systems in protecting shock- and vibration-sensitive equipment from near-fault ground motions and show the improvements associated with semi-active equipment isolation in terms of the mean and variability of the peak responses. Correlations between the isolation system variables and the responses provide guidance for improved behavior.

1. Introduction

The serviceability of hospitals, emergency-response centers, and data centers following an earthquake depend not only on the performance of the structural system, but also on the performance of the building contents. Passive isolation and damping systems have been shown to preserve structural integrity under demanding earthquakes [1–4]. Non-structural systems, and telecommunications equipment, however, can be particularly fragile to seismic effects and down-time costs of critical facilities can be measured in millions of dollars per minute [5–7]. In order to mitigate the seismic risk posed to equipment, isolation systems are commonly installed within data centers, hospitals, and emergency response centers. Typically these equipment isolation systems are a friction-pendulum, or rolling-pendulum type [8–10] with natural periods of 2–4 s. Passive equipment isolation systems perform extremely well during low-level seismic events [11–15]. During

*Corresponding author.
E-mail addresses: hpgavin@duke.edu (H.P. Gavin), anton.az@gmail.com (A. Zaicenco).
URL: http://www.duke.edu/~hpgavin/ (H.P. Gavin).

0022-460X/$ - see front matter © 2007 Elsevier Ltd. All rights reserved.
doi:10.1016/j.jsv.2007.05.039

high-amplitude, long-period, ground motions excessive isolator displacements could damage the isolators or overturn the equipment [11].

In long period isolation systems, increasing damping decreases isolator displacements but increases inertial loads sustained by the equipment. When the disturbance is poorly characterized, or highly variable, passive isolation systems may be enhanced by controllable damping, in which damping forces are regulated as a function of measured responses [16,17]. Such parametric (or semi-active) control systems are unconditionally stable, have modest power requirements, and can reduce vibration transmissibility for long period excitations without increasing the transmissibility for short periods [18,19].

This study focuses on the response of a semi-active isolation system to a set of different earthquakes. The analyses in this study involve structures of various configurations subjected to uni-directional ground motion, semi-active equipment isolation systems incorporating a new feedback control rule, and metamodeling to improve the computational efficiency of risk analysis computations.

2. Background

New results in the area of semi-active isolation effectively illustrate the performance of semi-active isolation in buildings [4,19–21] and bridges [22–24] subjected to multiple historic ground motions [23,25]. These studies contribute to the development of control algorithms (e.g., clipped optimal control [17] and clipped skyhook damping [26]) and controllable damping devices (e.g., magnetorheological dampers [17]). Semi-active control systems are nonlinear and the performance metrics commonly used in linear control analysis (frequency response functions or impulse response functions) cannot be obtained analytically. Furthermore, for earthquake engineering applications, the earthquake disturbance sources are transient and are not rich in frequency content. For these reasons, the analysis and design of semi-active control systems in earthquake engineering require transient response simulations of nonlinear dynamic systems. The reliability of semi-active isolation systems has not been systematically characterized because of the computational effort associated with transient response simulation.

In contrast to previous work on semi-active damping, as applied to buildings and bridges, this study addresses the application of semi-active damping to protect building contents from earthquake hazards. The primary goal of the study is to compare passive and semi-active equipment isolation systems by quantifying the performance benefits of semi-active equipment isolation systems in terms of probability density functions of peak responses. A new hybridization of the pseudo-negative stiffness control [27] and clipped skyhook control [16] algorithms is applied to equipment isolation systems within several multi-story building models. The selection of two parameters in this combined control governs the balance between response accelerations and isolator displacements. The damping and stiffness parameters of the passive and semi-active isolation systems are chosen to minimize equipment acceleration response without exceeding displacement limits. Comparing transient responses of these new systems to fixed base and base isolated buildings of four-to-seven stories, illustrates the advantages and the drawbacks of passive and semi-active control systems for protecting critical equipment from earthquake hazards.

Risk analysis is important for the assessment of new technologies for the protection of mission-critical subsystems. Response surfaces (metamodels) can significantly improve computational efficiencies to this end. Response surface approximations involve preliminary screening of the input variables, selection of the response surface polynomial order, and experiment design [28,29]. The convenient mathematical forms of response surface metamodels and their ability to be established from sparse data sets make them attractive for applications in design, optimization and risk analysis. Metamodeling can significantly increase the efficiency of risk estimation when failure probabilities are low. Response surface methods (RSM) have been successfully applied to several problems in structural dynamics. Failure probabilities of structures subject to short duration non-stationary earthquake loading have been estimated using stochastic finite elements and quadratic response surfaces [30]. Model updating for a nonlinear impact problem has been studied with response surfaces [31]. Metamodeling error estimation was studied in the context of a single-degree-of-freedom oscillator impacting a nonlinear material [32]. Response outputs were the peak acceleration and the time of arrival of this peak. Response surfaces were implemented for the purpose of damage identification from vibration data [33]. Uncertainties in input parameters (stiffness, mass, impulse magnitude and its location)

formed the input vector, while the studied outputs were peak displacements and natural frequencies. Polynomial response surfaces estimated by multiple regression were inverted as a damage detection algorithm. In order to determine if the outputs were indeed sensitive to some or all input parameters, preliminary variable screening was conducted before the RSM model was built. Variable screening significantly reduced the number of runs required to generate an adequate response surface model.

This study adopts quadratic stochastic response surface metamodels to alleviate the computational burden of determining peak response variability. Reliability analysis focuses on deriving the PDF's of the peak acceleration and displacement responses. The state limit function is dictated simply by non-exceeding acceleration or displacement threshold levels. Response variabilities are correlated to variability in parameters of the isolation system.

Following this introduction, Section 3 covers descriptions of the structural models, the earthquake ground motions, and the semi-active damping algorithm. Section 4 presents a parameter study of the damping and stiffness constants for passive and semi-active equipment isolation systems and compares acceleration and displacement responses for 16 different building types and four different earthquake ground motions in order to assess the expected performance improvement of the semi-active damping. Section 5 briefly reviews the stochastic response surface method and provides probability distribution functions of equipment acceleration and isolation displacement, and lists correlations of peak responses with the isolation system parameters. The results demonstrate how semi-active damping can reduce mean peak responses as well as peak response variances.

3. Structural models, excitation and semi-active control

The elements required to analyze and design a semi-active control system are a model of the system to be controlled, a set of transient excitation records, a model for a semi-active damping device, a parameterized control rule, a set of control objectives, and a well-designed passive control system for purposes of comparison. Because of the decisions required to develop and assemble these various elements, conclusions regarding semi-active control systems can sometimes be limited to the particular situation under study. In order to generalize findings, multiple cases are usually considered [25].

3.1. Structural models

The structural models used in this analysis are a set of 16 multi-story building frames with a light secondary system located on the first floor. The buildings range from four stories to seven stories, and each building model has four cases: (a) fixed-base without equipment isolation elements, (b) base isolated without equipment isolation elements, (c) fixed-base with a passive equipment isolation system, and (d) fixed-base with a semi-active equipment isolation system. The four cases of the four-story building model are illustrated in Fig. 1. The natural periods and modal damping ratios of the four fixed-base structural models, case (a), and the four

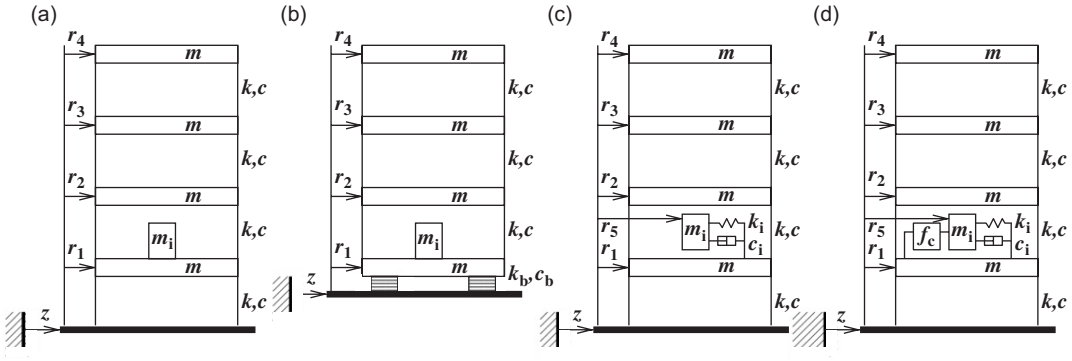

Fig. 1. Four cases of the four-story building models: (a) fixed base; (b) base isolated; (c) passive equipment isolation and (d) semi-active equipment isolation.

base-isolated building models, case (b), are given in Tables 1 and 2. Floor masses, m, are 680 tons each, the equipment mass, m_i, is 2 tons, the interstory stiffness, k, is 400 kN/mm, and the interstory damping rate, c, is 1.5 kN/mm/s. In case (b), the isolated building, k_b and c_b are adjusted to produce a first mode period of 2.5 s and a first mode damping ratio of 20%. Values of k_b range from 18 kN/mm for the four-story structure to 34 kN/mm for the seven-story structure. Values of c_b range from 2.9 kN/mm/s for the four-story structure to 6.4 kN/mm/s for the seven-story structure.

In cases (c) and (d) the equipment is isolated from the motions of the building structure via a compliant isolation system, with stiffness k_i and viscous damping c_i. In case (d), additional damping forces, f_c, between the secondary system and the first floor of the building may be regulated via a controllable damping device. The matrix equations of the motion for the structure, including the semi-active control forces, are:

$$\mathbf{M}\ddot{\mathbf{r}}(t) + \mathbf{C}\dot{\mathbf{r}}(t) + \mathbf{K}\mathbf{r}(t) + \mathbf{b}f_c(t) = -\mathbf{M}\mathbf{h}\ddot{z}(t), \tag{1}$$

where the vector $\mathbf{h} = [11 \ldots 11]^{\mathrm{T}}$ transmits ground acceleration, $\ddot{z}(t)$, to all degrees of freedom, the damper position vector $\mathbf{b} = [-10 \ldots 01]^{\mathrm{T}}$ applies the interstitial control force, f_c, between the first floor and the secondary system, which is the degree of freedom "$n+1$" in an n-story building.

3.2. Historical earthquake ground motions

The earthquake records are selected to represent a range of ground motions. They are: Imperial Valley—El Centro (1940) (PGA = 342 cm/s^2), Kobe–JMA (1995) (PGA = 617 cm/s^2), Northridge–Sylmar (1994) (PGA = 827 cm/s^2) and Loma-Prieta–Los Gatos (1989) (PGA = 559 cm/s^2). Velocity time histories and response spectra from these records are shown in Fig. 2. The response spectra illustrate the peak response

Table 1
Natural periods and damping ratios of the four-to-seven story base-isolated building models, case (a)

	Mode	1	2	3	4	5	6	7
Four story	Period, s	0.746	0.259	0.169	0.138			
	Damping	0.016	0.046	0.070	0.086			
Five story	Period, s	0.910	0.312	0.198	0.154	0.135		
	Damping	0.013	0.038	0.060	0.076	0.087		
Six story	Period, s	1.075	0.366	0.228	0.173	0.146	0.133	
	Damping	0.011	0.032	0.052	0.068	0.081	0.088	
Seven story	Period, s	1.239	0.419	0.260	0.194	0.160	0.142	0.132
	Damping	0.010	0.028	0.045	0.061	0.074	0.083	0.089

Table 2
Natural periods and damping ratios of the four-to-seven story base-isolated building models, case (b)

	Mode	1	2	3	4	5	6	7
Four story	Period, s	2.503	0.333	0.183	0.140			
	Damping	0.198	0.084	0.080	0.088			
Five story	Period, s	2.501	0.409	0.220	0.160	0.136		
	Damping	0.202	0.097	0.081	0.084	0.089		
Six story	Period, s	2.500	0.481	0.258	0.183	0.150	0.134	
	Damping	0.201	0.113	0.085	0.083	0.086	0.090	
Seven story	Period, s	2.500	0.546	0.294	0.206	0.165	0.144	0.133
	Damping	0.201	0.134	0.095	0.085	0.085	0.088	0.090

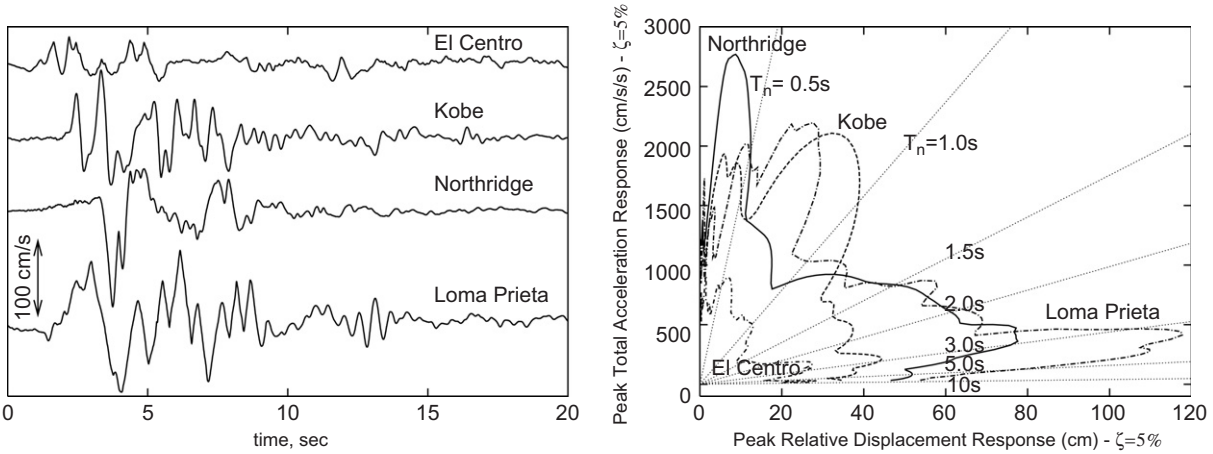

Fig. 2. Historical earthquake ground motions and response spectra, $\zeta = 5\%$.

accelerations and displacements of systems of different natural periods. The Northridge and Loma-Prieta records excite large displacement responses in systems with periods from 2 to 5 s and are selected because of the large displacement demands associated with these ground motions.

3.3. Negative stiffness and skyhook damping

The control method is a combination of pseudo-negative stiffness [27] and pseudo-skyhook damping [16]. In the negative stiffness method the control force, f_{ns}, opposes the stiffness forces in the isolation system, in an effort to reduce the coupling force across the isolation system

$$f_{\mathrm{ns}}(t) = -k_{\mathrm{ns}}\ \mathbf{b}^{\mathrm{T}}\mathbf{r}(t). \tag{2}$$

In the skyhook damping method the control force, f_{sd}, opposes the total velocity of the isolated system, in an effort to stabilize the secondary equipment with respect to an inertial reference frame

$$f_{\mathrm{sd}} = c_{\mathrm{sd}}(\dot{r}_i(t) + \dot{z}(t)), \tag{3}$$

where $\dot{r}_i(t) + \dot{z}(t)$ is the total velocity of the secondary system. The total control force is provided by a combination of skyhook damping and negative stiffness. The semi-active damper is an energy dissipation device; it cannot add mechanical energy to the structural system and may only exert dissipative forces. In order to satisfy the passivity constraint control forces must have the same sign as the velocity across the terminals of the device

$$f_c(t)\mathbf{b}^{\mathrm{T}}\ \dot{\mathbf{r}}(\mathbf{t}) > 0. \tag{4}$$

The desired (or target) control force, is then

$$f_t(t) = \begin{cases} f_{\mathrm{ns}}(t) + f_{\mathrm{sd}}(t) & \text{if } (f_{\mathrm{ns}}(t) + f_{\mathrm{sd}}(t))\mathbf{b}^{\mathrm{T}}\dot{\mathbf{r}}(t) > 0, \\ 0 & \text{otherwise.} \end{cases} \tag{5}$$

The semi-active device model used in this study incorporates actuator dynamics through a first-order time delay. The actual control force applied to the system, f_c, is given by

$$\dot{f}_c(t) = (f_t(t) - f_c(t))/T_d, \tag{6}$$

where T_d is a time-delay constant of 0.05 s.

Isolation systems for shock-sensitive equipment typically endeavor to minimize loads and accelerations sustained by the equipment without exceeding isolator displacement capacities. In this study, the isolator displacement capacity is 50 cm and accelerations below 50 $\mathrm{cm/s^2}$ are acceptable. The acceleration performance

metric is the peak total acceleration of the secondary system and is given by

$$A = \max_t |\ddot{z}(t) + \ddot{r}_i(t)|, \tag{7}$$

where $\ddot{r}_i(t)$ is the acceleration of the equipment with respect to the ground. The displacement performance metric is the peak relative displacement across the isolator system and is given by

$$D = \max_t |\mathbf{b}^{\mathrm{T}}\mathbf{r}(t)|. \tag{8}$$

As will be seen in the following sections, achieving acceptable acceleration responses within these displacement limitations is demanding, especially considering the transient and pulse-like nature of earthquake excitation, and requires equipment isolation periods longer than 6 s.

In the following section, values for the passive isolation parameters, k_i and c_i, and the semi-active control parameters, k_{ns} and c_{sd}, are selected in order to achieve a desirable balance between the total acceleration sustained by the isolated object and the displacements across the isolation system.

4. Parameter study for stiffness and damping values

The sensitivity of the performance metrics, A and D, to variations of the secondary isolation system parameters, k_i, c_i, k_{ns} and c_{sd}, are visualized in Figs. 3 and 4 as response surfaces over a range of parameter values. The five-story building model is used for these parameter studies.

The sensitivity study for the passive isolation system (parameters k_i and c_i) was conducted for $k_{\mathrm{ns}} = 0$ and $c_{\mathrm{sd}} = 0$, and is illustrated in Fig. 3. As expected, reducing the coupling between the equipment and the structure reduces the accelerations sustained by the equipment but increases the displacements in the isolation system. For the range of values investigated, peak response accelerations are not sensitive to changes in k_i but increase monotonically with c_i for all earthquake records except Loma-Prieta. Peak response displacements become large for larger values of k_i and smaller values of c_i.

The sensitivity study for the semi-active isolation system (parameters k_{ns} and c_{sd}) was conducted for $k_i = 2\,\mathrm{kN/m}$ and $c_i = 200\,\mathrm{N/m/s}$, and is illustrated in Fig. 4. Without semi-active forces, the period of this system is 6.3 s and the damping is 5%. Performance enhancements from semi-active damping increase with longer isolation periods and lower levels of passive damping [34]. Fig. 4 shows that a semi-active damping equipment isolation system can reduce accelerations and displacements below values achievable by passive isolation systems if the semi-active control constants k_{ns} and c_{sh} are selected properly. Semi-active response behavior can be excessive if the control constants are too large.

Performance metrics for building cases (a) and (b) (which do not involve the four isolation system parameters) are provided in Table 3 and provide a benchmark for the passive and semi-active equipment isolation systems. The peak isolation system response displacement, D, is not involved in these cases. In case (a), fixed-base, the peak response acceleration of the equipment is larger than, or as large as, the peak ground acceleration for almost all structures and all earthquakes. As the number of floors increases, and the natural periods increase, structures respond with smaller accelerations. Structural base isolation reduces the peak equipment acceleration by 50–70% as compared to the fixed base structures, depending on the earthquake. Response accelerations are nevertheless all well above the acceptable values of $50\,\mathrm{cm/s^2}$. Accelerations in the five-story fixed-base building are higher for all earthquakes except for the Loma-Prieta record.

Peak responses from a nominal passive isolation system with $k_i \approx 2\,\mathrm{kN/m}$ and $c_i \approx 1\,\mathrm{kN/m/s}$, $k_{\mathrm{ns}} = 0$, and $c_{\mathrm{sh}} = 0$ (6.3 s period and 25% critical damping) are shown in the third section of Table 3. The level of damping in case (c) was designed to keep the isolation system generally within the 50 cm displacement limit. The acceleration responses are larger than the acceptable level of $50\,\mathrm{cm/s^2}$ for the larger earthquakes, as shown in Table 3.

The fourth section of Table 3 shows peak responses from a semi-active isolation system with $k_i \approx 2\,\mathrm{kN/m}$, $c_i \approx 200\,\mathrm{N/m/s}$, $k_{\mathrm{ns}} \approx 3\,\mathrm{N/m}$, and $c_{\mathrm{sh}} \approx 200\,\mathrm{N/m/s}$ (6.3 s period and variable damping). For all four building structures and for all four earthquakes, semi-active control reduces response accelerations by 30–60% as compared to the passive isolation system while increasing response displacements by no more than 5%.

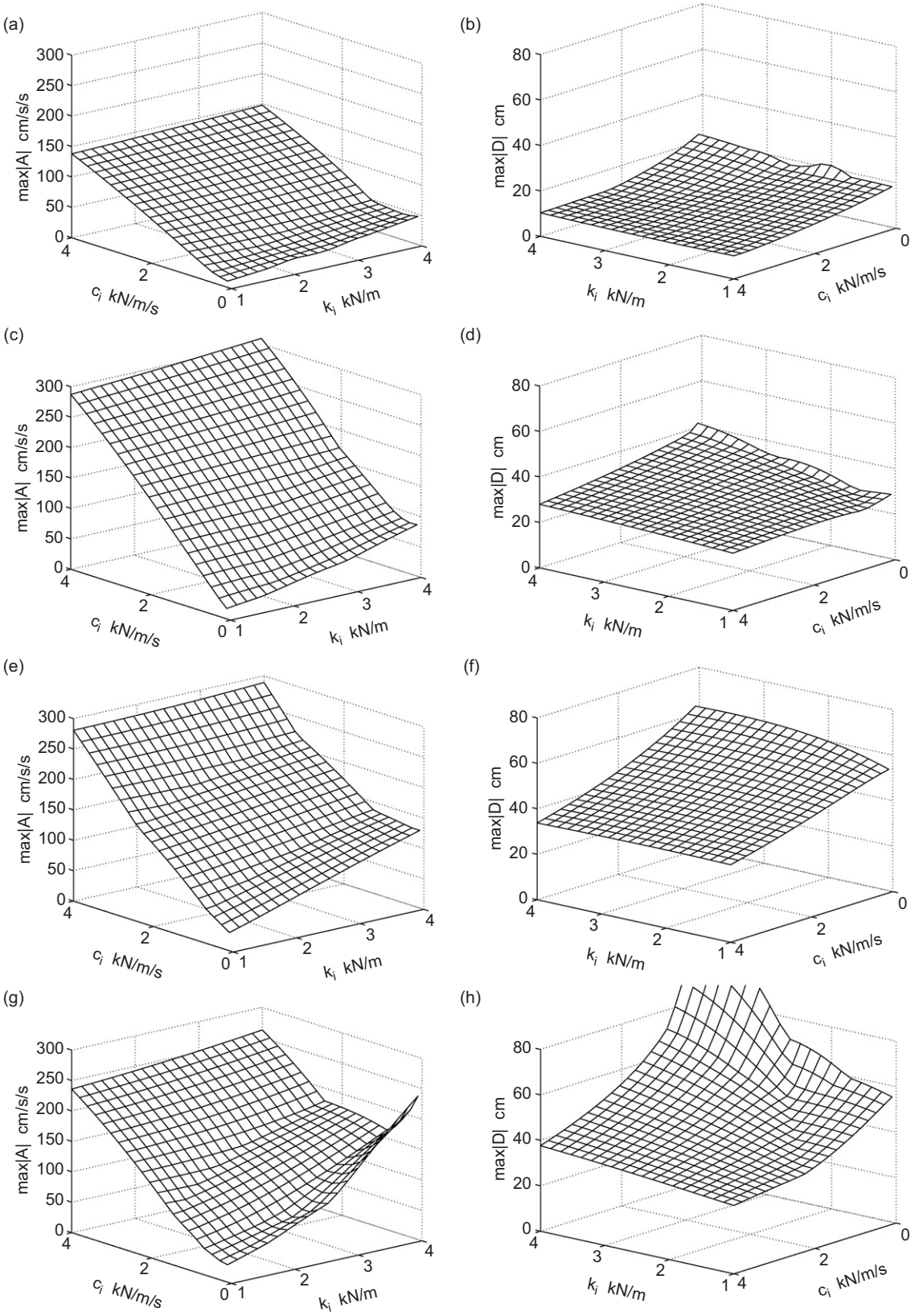

Fig. 3. Passive isolation system response as a function of isolation stiffness, k_i, and damping, c_i: (a, c, e, g) peak acceleration response A; (b, d, f, h) peak displacement response, D; (a, b) El Centro; (c, d) Kobe; (e, f) Northridge and (g, h) Loma-Prieta.

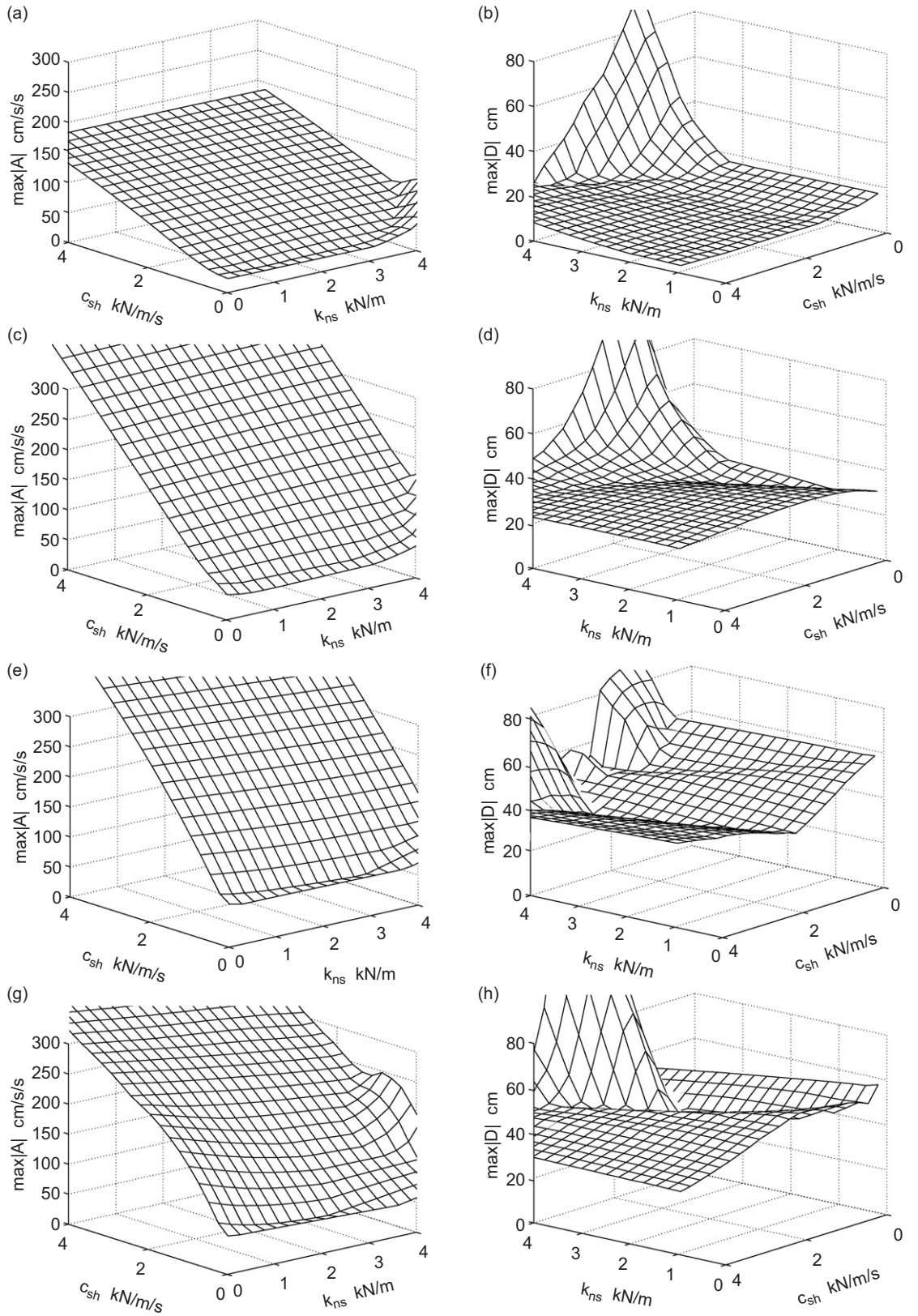

Fig. 4. Semi-active isolation system response as a function of negative stiffness gain, k_{ns}, and skyhook damping gain, c_{sh}: (a, c, e, g) peak acceleration response A; (b, d, f, h) peak displacement response, D; (a, b) El Centro; (c,d) Kobe; (e,f) Northridge and (g,h) Loma-Prieta.

Table 3
Peak values of total acceleration response, A (cm/s^2), and isolation displacement, D (cm), of the secondary system

Case	Floors	El Centro		Kobe		Northridge		Loma-Prieta	
		A	D	A	D	A	D	A	D
(a) Fixed-base[a]	4	441	–	1122	–	932	–	1562	–
	5	460	–	1414	–	1444	–	846	–
	6	433	–	935	–	1216	–	865	–
	7	343	–	838	–	890	–	807	–
(b) Base-isolated[a]	4	115	–	248	–	410	–	334	–
	5	134	–	267	–	449	–	356	–
	6	141	–	335	–	468	–	334	–
	7	174	–	359	–	463	–	355	–
(c) Passive equipment isolation[b]	4	40	17	81	30	101	48	112	52
	5	33	15	84	30	91	53	85	47
	6	32	14	82	34	91	53	92	48
	7	23	12	58	32	87	52	100	50
(d) Semi-active equipment isolation[b]	4	19	18	41	33	50	49	49	49
	5	24	23	38	37	57	56	48	47
	6	23	23	25	24	58	57	48	47
	7	23	23	33	31	57	56	48	46

[a]Peak values of response for the first floor.
[b]Peak values of response for isolated equipment at the first floor.

For the set of four historical earthquake ground motion selected for this study, the peak equipment responses from the fixed-base and base-isolated buildings (cases (a) and (b)) are more sensitive to the dynamics of the host structure than are the responses from the equipment isolation cases ((c) and (d)). The natural period and damping of the isolated equipment system are insensitive to the host-structure's dynamics, which explains the robustness of equipment isolation systems with regards to variability in the host-structure's dynamics.

Semi-active isolation systems with periods longer than 6.3 s tend to exhibit better performance, but for the sake of meaningful comparisons to the passive isolation system, the period was kept the same. The long isolation periods and low damping ratios of the passive components of the semi-active isolation system are critically important in achieving performance goals in semi-active damping [34].

Acceleration time-histories responses of the four-story structures to the Loma-Prieta earthquake are compared in Fig. 5. Passive equipment isolation (case (c)) reduces equipment accelerations by 60% as compared to the first floor accelerations of a passively base-isolated building (case (b)). Semi-active equipment isolation (case (d)) reduces equipment acceleration by an additional 50% as compared to the passive isolation system. The dashed line in Fig. 5(d) shows the semi-active damping force $f_c(t)$ divided by the equipment mass, m_i (2000 kg). This figure illustrates that the semi-active system provides a damping force that is roughly equal and opposite to the inertial forces (or the isolation shear force) on the equipment mass. Damping forces that oppose the inertial forces can reduce both equipment accelerations and isolator displacements. Fig. 5(e) and (f) show the passive and semi-active isolation system displacements.

Fig. 6 illustrates the hysteretic behavior of the semi-active forces in the isolation system (a), and the total forces in the isolation system (b). The semi-active isolation forces are essentially proportional to displacement and in phase with velocity whenever the passivity constraint is satisfied. The sum of the semi-active and passive isolation forces (i.e., the total base shear) are plotted in Fig. 6(b).

The analysis of this section shows that the peak accelerations sustained by equipment in buildings subjected to earthquakes can be significantly attenuated by isolation systems, that isolating the equipment itself can be more effective than isolating the entire building, and that semi-active equipment isolation can provide additional reductions, especially in accelerations. Comparisons of the peak response acceleration sustained by

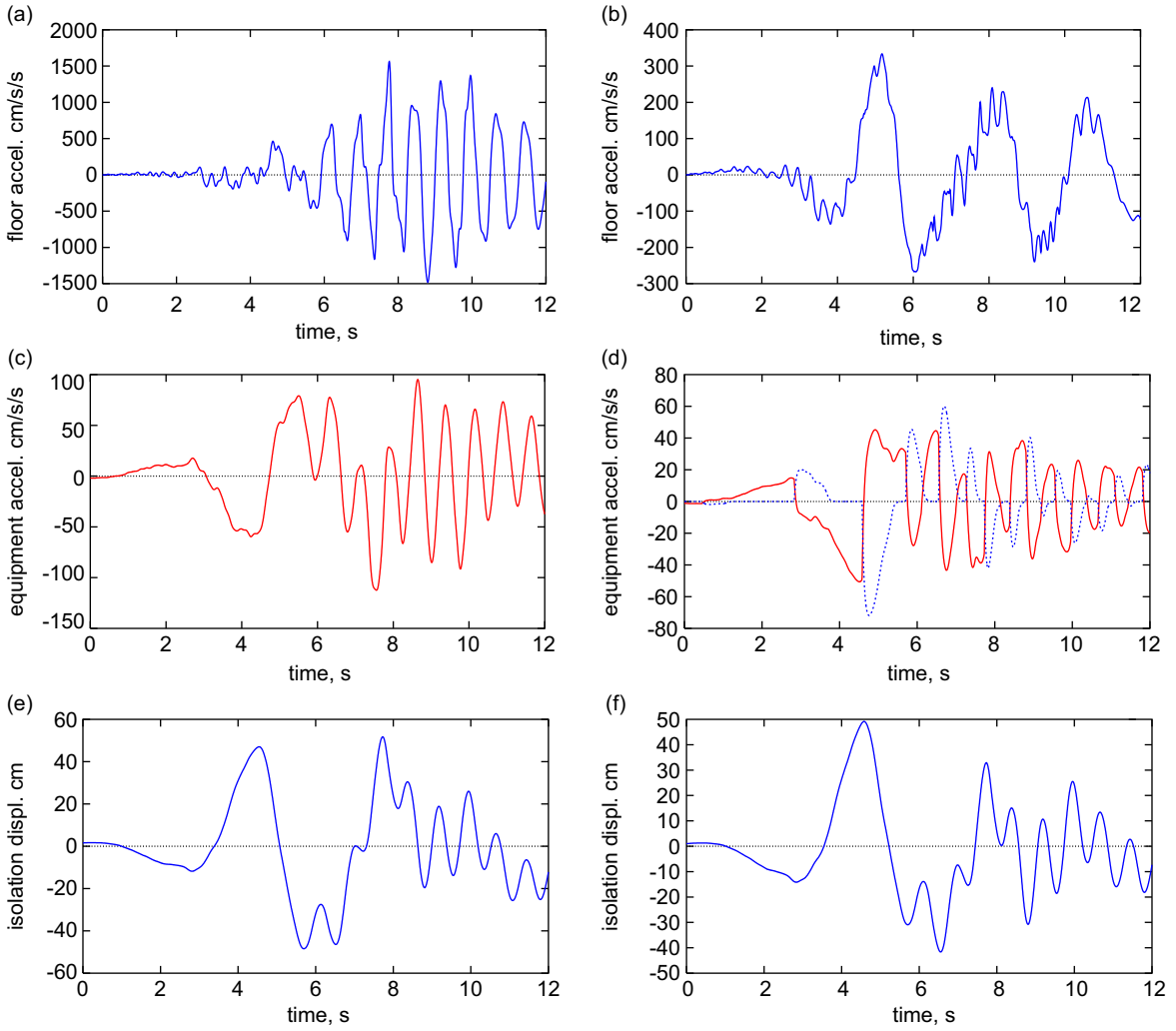

Fig. 5. (a)–(d) Equipment acceleration time histories for the four-story building models in response to the Loma-Prieta earthquake: (a) fixed-base; (b) base-isolated; (c) passive isolation; (d) semi-active isolation (- -: $\ddot{r}_{n+1}(t)+\ddot{z}(t)$, - -: f_c/m_i); (e) passive isolation system displacements and (f) semi-active isolation system displacements.

isolated equipment installed in buildings of various configurations (number of stories), and subjected to various earthquakes, show that the response is almost invariant to the number of stories. Because seismic risk has as much to do with mean values of the responses as it has to do with the variability of the responses, the reliability of the equipment isolation to variability in the isolation system parameters is analyzed next.

5. Risk analysis

Risk analysis is carried out using the stochastic response surface method (SRSM) [29] based on quadratic polynomial metamodels with uncertainties associated with parameters of the equipment isolation system. Although metamodels may be extended to approximate discontinuous surfaces [35]. Figs. 3 and 4 show that this is not necessary for the current study. The (SRSM) provides a closed-form approximation to the limit state function for the system under study and thereby reduces the computational effort of large Monte-Carlo analyses [28,29,36,37]. When the response surface is quadratic design points and failure probabilities may be evaluated analytically [38–41].

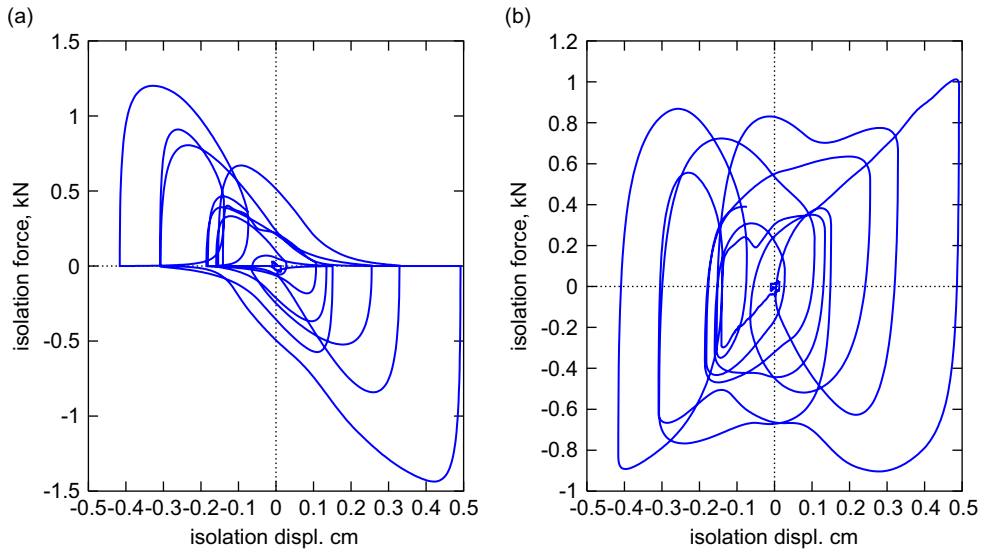

Fig. 6. (a) Semi-active damping force hysteresis and (b) semi-active damping force plus passive isolation force hysteresis.

5.1. Response surface metamodels

Response surface methods provide a means to establish computationally efficient approximations of detailed models with a relatively small number of detailed simulations [29]. Response surfaces are constructed using regression methods on sparse data obtained from more detailed analyses, resulting in polynomials relating the input variables to the corresponding responses or outputs. When the set of all possible input variables (the *design space*) is large and when resources are limited, experiment design methods help determine which detailed simulations should be executed [28,36].

The response surface is a mapping of n inputs $x_1,\ldots,x_n$ into m outputs, $y_1,\ldots,y_m$, using, for example, a quadratic polynomial form:

$$y_p(x) \approx a_p + \sum_{i=1}^{n} b_{pi}x_i + \sum_{i=1}^{n}\sum_{j=i}^{n} c_{pij}x_i x_j. \tag{9}$$

The coefficients (a_p, b_{pi}, and c_{pij}) are typically determined by singular value decomposition to fit the response surface to sparse data obtained from the detailed analysis.

5.2. The stochastic response surface method

The stochastic response surface method (SRSM) can be viewed as an extension of the classical deterministic response surface method (RSM). The main difference between the SRSM and the RSM is the representation of the design variables in the form of random variables. The SRSM assumes that square integrable random variables can be represented as functions of independent standardized random variables (SRV) [42]. The uncertain system's responses, or output variables, are expanded into a polynomial of the SRV's. As in RSM, only a limited number of detailed analyses are necessary to determine the SRSM. Uncorrelated input random variables, X_i, with CDF $F_i(X_i)$ are transformed to SRV's, ξ_i, through the use of the inverse standard Gaussian CDF, Φ^{-1},

$$\xi_i = \Phi^{-1}[F_i(X_i)], \tag{10}$$

and outputs are approximated by a polynomial expansion on ξ_i. The quadratic polynomial approximation is

$$Y \approx a + \sum_{i=1}^{n} b_i \xi_i + \sum_{i=1}^{n} \sum_{j=i}^{n} c_{ij} \xi_i \xi_j, \tag{11}$$

where Y is a random output of the model, a, b_i and c_{ij} are deterministic constants to be estimated. The least-squares method is employed to calculate polynomial coefficients in which the sum of squared residuals is

$$\chi^2 = \sum_{q=1}^{k} \left[y_q - \left(a + \sum_{i=1}^{n} b_i \xi_{qi} + \sum_{i=1}^{n} \sum_{j=i}^{n} c_{ij} \xi_{qi} \xi_{qj} \right) \right]^2, \tag{12}$$

where ξ_{qi} is the value of the ith SRV used in the qth simulation of the detailed model, and y_q is the result of a detailed simulation using the values ξ_{qi}. Setting partial derivatives equal to zero, $\partial(\chi^2)/\partial a = 0$, $\partial(\chi^2)/\partial b_i = 0$, $\partial(\chi^2)/\partial c_{ij} = 0$, the set of normal equations is obtained

$$\mathbf{y} = \mathbf{\Xi} \boldsymbol{\phi}, \tag{13}$$

where

$$\mathbf{y} = [y_1 \;\; y_2 \;\; \cdots \;\; y_q \;\; \cdots \;\; y_k]^{\mathrm{T}},$$

$$\mathbf{\Xi} = \begin{bmatrix} 1 & \xi_{11} & \xi_{12} & \cdots & \xi_{1n} & \xi_{11}\xi_{11} & \xi_{11}\xi_{12} & \cdots & \xi_{11}\xi_{1n} & \xi_{12}\xi_{12} & \xi_{12}\xi_{13} & \cdots & \cdots & \xi_{1n}\xi_{1n} \\ 1 & \xi_{21} & \xi_{22} & \cdots & \xi_{2n} & \xi_{21}\xi_{21} & \xi_{21}\xi_{22} & \cdots & \xi_{21}\xi_{2n} & \xi_{22}\xi_{22} & \xi_{22}\xi_{23} & \cdots & \cdots & \xi_{2n}\xi_{2n} \\ \vdots & \vdots & \vdots & \cdots & \vdots & \vdots & \vdots & \cdots & \vdots & \vdots & \vdots & \cdots & \cdots & \vdots \\ 1 & \xi_{q1} & \xi_{q2} & \cdots & \xi_{qn} & \xi_{q1}\xi_{q1} & \xi_{q1}\xi_{q2} & \cdots & \xi_{q1}\xi_{qn} & \xi_{q2}\xi_{q2} & \xi_{q2}\xi_{q3} & \cdots & \cdots & \xi_{qn}\xi_{qn} \\ \vdots & \vdots & \vdots & \cdots & \vdots & \vdots & \vdots & \cdots & \vdots & \vdots & \vdots & \cdots & \cdots & \vdots \\ 1 & \xi_{k1} & \xi_{k2} & \cdots & \xi_{kn} & \xi_{k1}\xi_{k1} & \xi_{k1}\xi_{k2} & \cdots & \xi_{k1}\xi_{kn} & \xi_{k2}\xi_{k2} & \xi_{k2}\xi_{k3} & \cdots & \cdots & \xi_{kn}\xi_{kn} \end{bmatrix},$$

$$\boldsymbol{\phi} = [a \;\; b_1 \;\; b_2 \;\; \ldots \;\; b_n \;\; c_{11} \;\; c_{12} \;\; \ldots \;\; c_{1n} \;\; c_{22} \;\; c_{23} \;\; \cdots \;\; \cdots \;\; c_{nn}]^{\mathrm{T}} \tag{14}$$

in which a sparse data set, $\mathbf{y}$, from the detailed model is evaluated for k different sets of the n SRV's, $\xi_{q1}, \ldots, \xi_{qn}$, $q = 1, \ldots, k$. For problems involving $m > 1$ output variables, Eq. (15) would be evaluated m times producing m sets of the polynomial coefficients, a, b_i, c_{ij}. The Vandermode matrix $\mathbf{\Xi}$ can be the same for all m normal equations. The number of elements, k, in the sparse data set, $\mathbf{y}$, must not be less than the total number of coefficients

$$k \geqslant 1 + 2n + \frac{n!}{2(n-2)!}. \tag{15}$$

Once the coefficients are known, many samples of the output variables can be estimated easily from Eq. (11) or Eq. (13). This is essentially the same as running Monte-Carlo analysis on the metamodel approximation of the original system. The resulting samples of the system outputs may then be analyzed using standard statistical methods.

5.3. Effect of variability of passive and semi-active control parameters

In this study reliability analysis is focused on deriving the PDF's and correlations for the peak total acceleration of the secondary system, A, and the peak isolator displacement, D. The PDF's, $f_A(a)$ and $f_D(d)$, and correlations are compared for passive isolation and semi-active isolation. The limit state function is dictated simply by non-exceeding threshold levels $a_{\max} = 50\,\mathrm{cm/cm^2}$ and $d_{\max} = 50\,\mathrm{cm}$, and the probability of failure is

$$P_f = \mathrm{Prob}[A > a_{\max} \cup D > d_{\max}]. \tag{16}$$

To study the effects of variations in the passive isolation parameters, c_i and k_i, on A and D, the input variables, k_i and c_i, are assumed to be log-normal with mean values $\mu_{k_i} = 2000\,\mathrm{N/m}$ and $\mu_{c_i} = 1000\,\mathrm{N/m/s}$,

and coefficients of variation $V_{k_i} = 0.1$ and $V_{c_i} = 0.3$. It is presumably more difficult to accurately provide the designed damping level than the designed stiffness in the isolation system. The coefficients of variation were selected to be large enough to reveal meaningful correlations between the isolation system parameters and the responses.

Eq. (13) was solved using singular-value decomposition for the two sets of the six polynomial coefficients, a, b_1, b_2, c_{11}, c_{12}, and c_{22}; one set for the response surface for A, and the other set for the response surface for D. This procedure was repeated for each of the four historical earthquake records, El Centro, Kobe, Northridge and Loma-Prieta.

Mean and standard deviations of the peak responses and correlations with the input random variables, k_i and c_i, are provided in Table 4. For the selected range of values of k_i and c_i, the passive isolation systems are almost certain to exceed the threshold values selected when responding to strong ground motions. Peak

Table 4
Statistics of the response variables A and D with respect to uncertainty in the passive control parameters: $\mu_{k_i} = 2000\,\mathrm{N/m}$, $\mu_{c_i} = 1000\,\mathrm{N/m/s}$, $V_{k_i} = 0.1$, $V_{c_i} = 0.3$

Parameter	El Centro	Kobe	Northridge	Loma-Prieta	Units
μ_A	36	86	95	83	$\mathrm{cm/s^2}$
σ_A	11	21	17	16	$\mathrm{cm/s^2}$
μ_D	15	30	53	48	cm
σ_D	1	1	2	4	cm
P_f	0.11	≈ 1	≈ 1	≈ 1	–
$\rho_{A,D}$	−0.95	−0.25	−0.80	−0.48	–
ρ_{A,k_i}	0.02	0.02	0.23	0.38	–
ρ_{A,c_i}	0.97	0.99	0.87	0.91	–
ρ_{D,k_i}	−0.12	0.95	0.16	0.28	–
ρ_{D,c_i}	−0.99	−0.28	−0.98	−0.60	–

Table 5
Statistics of the response variables A and D with respect to uncertainty in the passive and semi-active control parameters: $\mu_{k_i} = 2000\,\mathrm{N/m}$, $\mu_{c_i} = 200\,\mathrm{N/m/s}$, $\mu_{k_{\mathrm{ns}}} = 3000\,\mathrm{N/m}$, $\mu_{c_{\mathrm{sh}}} = 200\,\mathrm{N/m/s}$, $V_{k_i} = 0.1$, $V_{c_i} = 0.3$, $V_{k_i} = 0.1$, $V_{c_i} = 0.1$

Parameter	El Centro	Kobe	Northridge	Loma-Prieta	Units
μ_A	20	37	60	51	$\mathrm{cm/s^2}$
σ_A	5	4	6	7	$\mathrm{cm/s^2}$
μ_D	19	32	55	48	cm
σ_D	3	4	1	2	cm
P_f	0.001	0.01	≈ 1	0.50	–
$\rho_{A,D}$	0.58	0.42	0.53	0.60	–
ρ_{A,k_i}	0.17	0.21	0.97	0.82	–
ρ_{A,c_i}	0.10	0.63	0.28	−0.01	–
ρ_{D,k_i}	−0.46	−0.40	0.66	0.77	–
ρ_{D,c_i}	−0.06	−0.08	−0.49	−0.31	–
$\rho_{A,k_{\mathrm{ns}}}$	0.25	0.31	0.04	0.07	–
$\rho_{A,c_{\mathrm{sh}}}$	−0.02	0.10	−0.06	0.02	–
$\rho_{D,k_{\mathrm{ns}}}$	0.42	0.41	−0.18	−0.50	–
$\rho_{D,c_{\mathrm{sh}}}$	0.02	−0.03	−0.26	−0.15	–

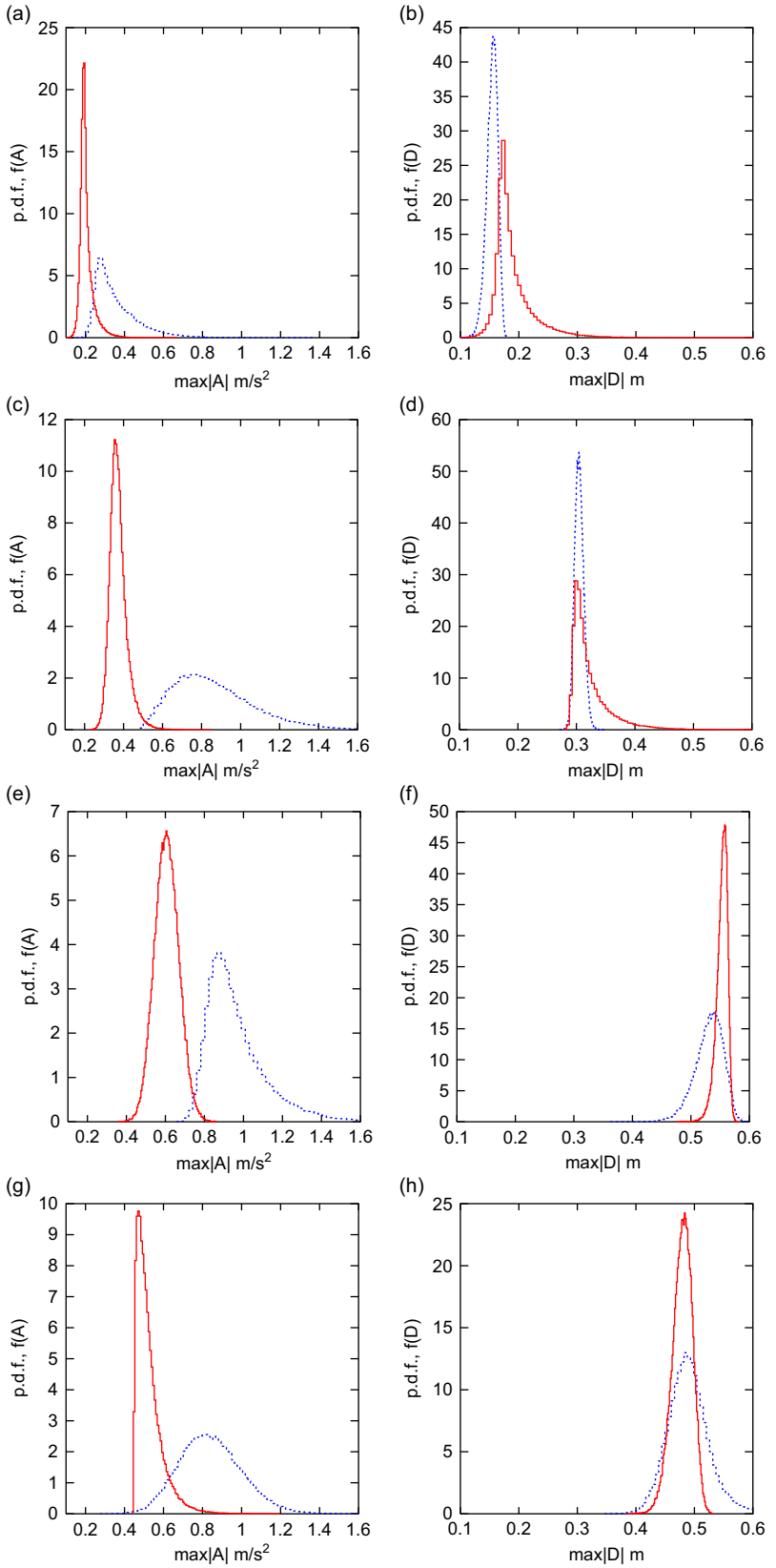

Fig. 7. Probability density functions from Monte-Carlo sampling of the response surface. Dashed lines: passive, Solid lines: semi-active: (a, c, e, g) A; (b, d, f, h) D; (a, b) El Centro; (c,d) Kobe; (e,f) Northridge and (g, h) Loma-Prieta.

response accelerations, A, are negatively correlated with peak response displacements, D. The isolation damping, c_i, is positively correlated with the peak response acceleration, A, and is negatively correlated with peak response displacements, D. Decreasing c_i decreases A but increases D for all four earthquakes. Correlations with k_i depend on the earthquake.

To study the effects of variations in both the passive and semi-active isolation parameters on A and D, the input variables are assumed to be log-normal with mean $\mu_{k_i} = 2000\,\mathrm{N/m}$, $\mu_{c_i} = 200\,\mathrm{N/m/s}$, $\mu_{k_{\mathrm{ns}}} = 3000\,\mathrm{N/m}$, and $\mu_{c_{\mathrm{sh}}} = 200\,\mathrm{N/m/s}$, and coefficients of variation $V_{k_i} = 0.1$, $V_{c_i} = 0.3$, $V_{k_{\mathrm{ns}}} = 0.1$, and $V_{c_{\mathrm{sh}}} = 0.1$.

Mean values, standard deviations, and correlations for the set of four earthquakes are provided in Table 5. The semi-active isolation system is much less likely to exceed the threshold limits. The semi-active isolation outperforms the passive isolation of secondary system for the four historical earthquakes, providing much smaller values of acceleration response, with respect to uncertainties in k_i, c_i, k_{ns}, and c_{sh}. The semi-active isolation application results in peak acceleration response statistics with mean values that are half those of the passive isolation system. Moreover, the standard deviations of the peak acceleration response with semi-active isolation are only 10–40% of those with passive isolation.

With semi-active damping, peak response accelerations are now positively correlated with peak response displacements, indicating that further reductions in A would also tend to result in smaller values of D. For the four earthquakes A is positively correlated with k_i and for the Northridge and Loma-Prieta earthquakes D is positively correlated with k_i. Correlations of A and D with the other parameters are not as strong or systematic; the most effective way to reduce both A and D is therefore to design semi-active isolation systems with very long natural periods (longer than 6 s, if possible). For the selected data range, increasing c_i tends to reduce D at the expense increasing A.

Probability density functions of A and D for the passive and semi-active equipment isolation systems are given in Fig. 7 and show the effect that semi-active damping has in reducing both the mean and the variance of peak responses [43]. For all response surfaces the condition number of $\boldsymbol{\Xi}$ was less than 20 and R^2

$$R^2 = 1 - \|\mathbf{y} - \boldsymbol{\Xi}\boldsymbol{\phi}\|_2^2 / \|\mathbf{y} - \bar{\mathbf{y}}\|_2^2, \tag{17}$$

was greater than 95%. The PDF's of A and D were evaluated with 100,000 Monte-Carlo samples of the response surface models. The number of Monte-Carlo simulations was large enough to capture the sharp tails of some of the distributions shown in Fig. 7. These distributions were calculated using less than 100 simulations of the detailed model, corresponding to a speed-up factor of more than 1000.

6. Conclusions

Properly designed semi-active isolation systems, applied to the protection of light equipment within buildings, can significantly reduce the peak response accelerations without substantially increasing isolator displacements, in comparison with well-designed passive equipment isolation systems.

Application of the stochastic response surface metamodels for reliability analysis of semi-active control systems illustrates the benefits of semi-active control in terms of mean responses and response variances. Semi-active damping reduces peak response accelerations by 30–60% and reduces peak acceleration variances by 60–90% as compared to a well-designed passive isolation system. The ability of semi-active isolation to reduce both acceleration and displacement responses tends to increase with the natural period of the isolation system.

The stochastic response surface method is an accurate and effective tool in estimating response statistics and in this analysis it provided a speed-up factor of over 1000.

Future work will address reliability due to variability in ground motion parameters, bi-directional ground motion, equipment with mass eccentricity, experimental implementation, and GIS-based loss estimation for vibration-sensitive equipment installations.

Acknowledgments

The authors gratefully acknowledge support from the US Civilian Research & Development Foundation for the Independent States of the Former Soviet Union (CRDF) under Award No. MG1-2319-CH-02 and from the National Science Foundation under Award No. NSF-0704959.

References

[1] C. Alhan, H. Gavin, A parametric study of linear and non-linear passively damped seismic isolation systems for buildings, *Engineering Structures* 26 (4) (2004) 485–497.
[2] J.M. Kelly, *Earthquake-Resistant Design with Rubber*, second ed., Springer, London, 1997.
[3] J.M. Kelly, The role of damping in seismic isolation, *Earthquake Engineering and Structural Dynamics* 28 (1) (1999) 3–20.
[4] S. Nagarajaiah, X. Sun, Response of base-isolated USC hospital building in Northridge Earthquake, *Journal of Structural Engineering* 126 (10) (2000) 1177–1186.
[5] T.F. Armistead, Splendid isolation, *Engineering News-Record* 243 (11) (1999) 52.
[6] K. Maddox, F. Wallen, Mission critical facilities—a 21st century challenge, *Washington Business Journal*, December 8, 2000.
[7] J. Press, M. Betts, J. Ngo, M. Cantwell , A program for successful testing of network equipment building systems, *Compliance Engineering*, July–August 2000.
[8] A. Kasalanati, A.M. Reinhron, M.C. Constantinou, D. Sanders, Experimental study of ball-in-cone isolation system, *Proceedings of the ASCE Structures Congress XV*, April 13–16 1997, pp. 1191–1195.
[9] Z.A. Kemeny, Ball-in-cone seismic isolation bearing, U.S. Patent 5599106, February 4, 1997.
[10] B. Myslimaj, S. Gamble, D. Chin-Quee, A. Davies, Base isolation technologies for seismic protection of museum artifacts, *The 2003 IAMFA Annual Conference in San Francisco*, California September 21–24, 2003.
[11] H.P. Gavin, C. Alhan, Reliability of base-isolation for the protection of critical facilities from earthquake hazards, *Engineering Structures* 27 (9) (2005) 1435–1449.
[12] W.D. Iwan, The earthquake design and analysis of equipment isolation systems, *Earthquake Engineering and Structural Dynamics* 6 (1978) 523–534.
[13] Y.L. Xu, H.J. Liu, Z.C. Yang, Hybrid platform for vibration control of high-tech equipment in buildings subject to ground motion part 1: experiment, *Earthquake Engineering and Structural Dynamics* 32 (2003) 11851200.
[14] Y.L. Xu, B. Li, Hybrid platform for high-tech equipment protection against earthquake and microvibration, *Earthquake Engineering and Structural Dynamics* 35 (2006) 943967.
[15] J.N. Yang, A.K. Agrawal, Protective systems for high-technology facilities against microvibration and earthquake, *Structural Engineering and Mechanics* 10 (6) (2000) 561–575.
[16] D. Karnopp, M.G. Crosby, R.A. Harwood, Vibration control using semi-active force generators, *Journal of Engineering for Industry* 96 (2) (1974) 619–627.
[17] B.F. Spencer Jr., M.K. Sain, Controlling buildings: a new frontier in feedback, *IEEE Control Systems Magazine* 17 (6) (1997) 19–35.
[18] H.P. Gavin, U. Aldemir, C. Alhan, Optimal semi active isolation, *Journal of Engineering Mechanics* 132 (7) (2006) 705–713.
[19] G.W. Housner, L.A. Bergman, T.K. Caughey, A.G. Chassiakos, R.O. Claus, S.F. Masri, R.E. Skelton, T.T. Soong, B.F. Spencer, J.T.P. Yao, Structural control: past, present, and future, *Journal of Engineering Mechanics* 123 (9) (1997) 897–971.
[20] N. Wongprasert, M.D. Symans, Experimental evaluation of adaptive elastomeric base-isolated structures using variable-orifice fluid dampers, *Journal of Structural Engineering* 131 (6) (2005) 867–877.
[21] O. Yoshida, S.J. Dyke, Response control of full-scale irregular buildings using magnetorheological dampers, *Journal of Structural Engineering* 131 (5) (2005) 734–742.
[22] R.E. Christenson, B.F. Spencer, E.A. Johnson, Experimental verification of smart cable damping, *Journal of Engineering Mechanics* 132 (3) (2006) 268–278.
[23] S.J. Dyke, J.M. Caicedo, G. Turan, L.A. Bergman, S. Hague, Phase I benchmark control problem for seismic response of cable-stayed bridges, *Journal of Structural Engineering* 129 (7) (2003) 857–872.
[24] S.S. Sahasrabudhe, S. Nagarajaiah, Semiactive control of sliding isolated bridges using MR dampers: an experimental and numerical study, *Earthquake Engineering and Structural Dynamics* 34 (8) (2005) 965–983.
[25] S. Narasimhan, S. Nagarajaiah, E.A. Johnson, H.P. Gavin, Smart base-isolated benchmark building part I: problem definition, *Journal of Structural Control and Health Monitoring* 13 (1–2) (2006) 573–588.
[26] H.P. Gavin, Control of seismically-excited vibration using electrorheological materials and Lyapunov methods, *IEEE Transactions on Control Systems Technology* 9 (1) (2001) 27–36.
[27] H. Iemura, A. Igarashi, M.H. Pradono, A. Kalantari, Negative stiffness friction damping for seismically isolated structures, *Journal of Structural Control* 13 (2003) 775–791.
[28] G.E.P. Box, N.R. Draper, *Empirical Model—Building and Response Surfaces*, Wiley, New York, NY, 1987.
[29] R.H. Myers, D.C. Montgomery, *Response Surface Methodology*, Wiley, New York, NY, 1995.
[30] J. Huh, A. Haldar, Stochastic finite-element-based seismic risk of nonlinear structures, *Journal of Structural Engineering* 127 (3) (2001) 323–329.
[31] F.M. Hemez, A.C. Wilson, S.W. Doebling, Design of computer experiments for improving an impact test simulation, *19th International Modal Analysis Conference*, Kissimmee, FL, 2001.
[32] R. Shinn, F.M. Hemez, S.W. Doebling, Estimating the error in simulation prediction over the design space, *Proceedings of the 44th AIAA/ASME/ASCE/AHS Structures, Structural Dynamics, and Materials Conference*, Norfolk, VA, 2003.
[33] M. Cundy, Response Surface Analysis and its Applications to Structural Dynamics Problems, PhD Thesis, Virginia Tech., 2003.
[34] H.P. Gavin, C. Alhan, Guidelines for low-transmissibility semi-active vibration isolation, *Smart Materials and Structures* 14 (2) (2005) 297–306.

[35] M. Meckesheimer, R.R. Barton, T. Simpson, F. Limayem, B. Yannou, Metamodeling of combined discrete/continuous responses, *AIAA Journal* 39 (10) (2001) 1950–1959.
[36] G.E.P. Box, W.G. Hunter, J.S. Hunter, *Statistics for Experimenters: An Introduction to Design, Data Analysis and Model Building*, Wiley, New York, 1978.
[37] T. Krishnamurthy, V.J. Romero, Construction of response surface with higher order continuity and its application to reliability engineering, *AIAA-2002-1466, 43rd AIAA/ASME/ASCE/AHS/ASC Structures, Structural Dynamics, and Material Conference*, Denver, April 22–25, 2002.
[38] K. Breitung, L. Faravelli, Response surface methods and asymptotic approximations, in: F. Casciati, B. Roberts (Eds.), *Mathematical Models for Structural Reliability Analysis*, CRC Press, Boca Raton, FL, 1996.
[39] L. Faravelli, Response surface approach for reliability analysis, *Journal of Engineering Mechanics* 115 (12) (1989) 2763–2781.
[40] S. Gupta, C.S. Manohar, An improved response surface method for the determination of failure probability and importance measures, *Structural Safety* 26 (2004) 123–139.
[41] L. Olivi, Response surface methodology in risk analysis, in: G. Apostolakis, S. Garribba, G. Volta (Eds.), *Synthesis and Analysis Methods for Safety and Reliability Studies*, Plenum Press, New York, 1980.
[42] M.A. Tatang, Direct Incorporation of Uncertainty in Chemical and Environmental Engineering Systems, PhD Thesis, Massachusetts Institute of Technology, 1995.
[43] Y.F. Zhang, W.D. Iwan, Statistical performance analysis of seismic-excited structures with active interaction control, *Earthquake Engineering and Structural Dynamics* 32 (2003) 1039–1054.